An Experimental Investigation of the Dynamic Response of Bladeless Vortex-Induced Vibration Turbines Using Novel Materials in a Wind Tunnel

Ahmed Ketata
Laboratory of Electromechanical Systems, National Engineering School of Sfax, University of Sfax, Sfax, Tunisia | Preparatory Institute for Engineering Studies of Gabes, University of Gabes, Gabes, Tunisia
ketata.ahmed.enib@gmail.com (corresponding author)

Lina Chelbi
Laboratory of Electromechanical Systems, National Engineering School of Sfax, University of Sfax, Sfax, Tunisia
lina.chelbi@enis.tn

Hasna Abid
Laboratory of Electromechanical Systems, National Engineering School of Sfax, University of Sfax, Sfax, Tunisia
hasna.abid@enit.utm.tn

Zied Driss
Laboratory of Electromechanical Systems, National Engineering School of Sfax, University of Sfax, Sfax, Tunisia
zied.driss@enis.tn

Received: 22 May 2025 | Accepted: 13 July 2025

 DOI: https://doi.org/10.48084/etasr.12314

ABSTRACT

This study presents an experimental investigation into the vibration characteristics of four different Vortex Bladeless Wind Turbine (VBWT) prototypes made with different mast materials - Glass Fiber (GF), Polyurethane (PU), and Polyethylene (PE) - and rod lengths. They were tested in a wind tunnel with different Reynolds number flow regimes using two rod lengths (60 mm and 90 mm) to evaluate their performance under controlled conditions. An acquisition system based on Arduino was constructed to measure the linear acceleration of the vibration of each prototype. The experimental results revealed that the rod length had a significant impact on both the amplitude and frequency of vibration, with longer rods producing greater deflection and lower natural frequencies. The mast diameter was also found to influence the frequency, with larger diameters yielding reduced vibration frequencies. Furthermore, the material of the mast played a crucial role in the dynamic behavior. The PU mast exhibited the highest vibration amplitudes and frequencies due to its lower mass and greater flexibility, compared to the GF and PE configurations. These findings contributed to the advancement of this emerging renewable energy technology of VBWTs.

Keywords-Vortex Bladeless Wind Turbines (VBWTs); Vortex-Induced Vibration (VIV); renewable energy; wind tunnel; polyurethane; glass fiber; polyethylene; FFT spectrum analysis

I. INTRODUCTION

Due to the population growth and rapid development in several countries, the global energy demand is increasing steadily [1]. The environmental impact of conventional energy systems is significant, mostly due to the Greenhouse Gas (GHG) emissions resulting from fossil fuel combustion. These emissions trap heat in the Earth's atmosphere, causing ecosystem disruptions, rising sea levels, and extreme weather events [2]. As a result, the field of renewable energy sources, such as geothermal, biomass, solar, wind, and hydropower, has made significant advances [3].

Wind energy is commonly generated using two main types of turbines: horizontal-axis and vertical-axis designs. Despite their effectiveness, these systems face challenges, mainly due to their large size, including visual intrusion, noise pollution, and transportation difficulties, which limit their use in densely populated or ecologically sensitive areas. Conversely, the wind turbines with a small size often become economically unfeasible compared to other energy sources or land uses, thus finding their main applications in small-scale power generation.

The growing interest in wind power has spurred the development of various turbine designs, in order to optimize the energy harvesting efficiency [4]. One such innovation is the Bladeless Wind Turbine (BWT), which offers a promising approach to capturing the wind energy. This design operates according to the principle of Vortex-Induced Vibration (VIV), where the mast oscillates as the wind flows around it, creating vortices. The resulting vibrations generate kinetic energy, which is then converted into electricity through a linear generator, like those used in [5] for capturing the wave energy.

Several studies have investigated the effectiveness of BWTs. Specifically, authors in [6] examined the dynamic modeling of four configurations of a BWT, which differed in the cylinder shape and its mounting structure. BWT1 was a right circular flexible cylinder, BWT2 was a conic flexible cylinder, BWT3 was a right circular rigid cylinder mounted on a flexible beam, and BWT4 was a conic rigid cylinder mounted on a flexible beam. In [7], five distinctive geometries were analyzed: a traditional circular form, a decagonal form, and three sinusoidal forms. Authors in [8] used ANSYS software and Computational Fluid Dynamic (CFD) analysis to simulate the vortex behavior and its impact on the turbine performance. The findings underscored the importance of incorporating natural frequencies and vibration modes in minimizing the excessive oscillations that might risk the turbine's structural integrity. Authors in [9] examined the effect of the amplitude-to-diameter ratio on vortex-induced vibrations using CFD simulations, finding that changes in Reynolds number significantly affect the displacement and aerodynamic forces. Similarly, authors in [10] examined vertical mast configurations with different taper ratios, while in [11], CFD analysis was utilized to assess the design parameters affecting the efficiency, such as the lift and drag coefficients and vortex shedding frequency.

Authors in [12] conducted wind tunnel experiments comparing rectangular and circular cross-sections. Their results indicated that the resonance reduced velocity was approximately 3.7 for the rectangular prism and 4.0 for the circular cylinders. The depth of the rectangular prism had a linear relationship with the displacement rate and vibration frequency of the test models, directly influencing the power generation output. Additionally, authors in [13] examined how material stiffness affected the turbine efficiency, displacement, and power generation, revealing that the damping and flexibility have a major impact on energy conversion. In [14], the performance of Vortex Bladeless Wind Turbines (VBWTs) was improved by modifying the mast design to ensure uniform vortex shedding frequencies along its height. Numerical simulations were conducted to analyze the effect of vortex shedding frequency on an oscillating structure, introducing a characteristic length that varied depending on the wind speed and structural oscillations. The findings showed that the Reynolds number had a considerable impact on the vortex shedding behavior. Authors in [15], introduced a small-scale BWT using a Magnetorheological Elastomer (MRE) to adjust the structural frequency. By applying a magnetic field, the resonant frequency could shift by 64.3%, expanding the operational wind speed range from 2.0 m s^{-1} to 3.3 m s^{-1}. The experiments demonstrated that maintaining resonance within the lock-in range significantly enhanced the energy harvesting efficiency.

Overall, the VBWT seems to be an innovative approach to wind energy generation, utilizing vortex-induced vibrations instead of traditional rotating blades. Although numerous studies have numerically investigated the key parameters affecting the efficiency of these turbines, experimental studies on this topic remain limited. In this context, the current study presents a detailed experimental analysis of four BWTs with different mast's material as well as varying rod lengths for a wide range of Reynolds number. The novelty of this study lies in the investigation of mast materials, specifically GF, PU, and PE, which have not been previously examined or directly compared. Through this approach, the goal is to confirm the operational characteristics of the BWT while looking for an optimal design allowing the maximum of energy harnessing.

II. MATERIALS AND METHODS

To investigate the impact of the material properties on the vibrational behavior of VBWTs, multiple prototypes were manufactured using different mast materials. The selected materials were PU, PE, and GF. PU is known for its lightness and flexibility, while PE is a dense, resilient plastic with good elasticity. GF, a lightweight composite, is recognized for its rigidity. Each mast had a cylindrical shape and was fixed to a stainless-steel rod shell, which acted as the base support and transmitted vibrations to the whole system. The turbine prototypes followed a standard nomenclature - VBWT-M-D-L-l, where VBWT stands for the Vortex Bladeless Wind Turbine, M represents the mast material (PU, PE or GF), D is the mast diameter (mm), L is the mast height (mm), and l is the length of the rod given in mm.

Figure 1 illustrates the manufactured VBWT prototypes with different mast materials, diameters, and heights. Specifically:

- VBWT-GF-14-190: a GF mast with a diameter of 14 mm and a height of 190 mm.
- VBWT-PU-14-190: a PU mast with a diameter of 14 mm and a height of 190 mm.
- VBWT-PU-28-165: a PU mast with a diameter of 28 mm and a height of 165 mm.
- VBWT-PE-11-260: a PE mast with a diameter of 11 mm and a height of 260 mm.

The choice of the mast dimensions for each material depended on the limitations of the available manufacturing processes. In this study, two rod lengths were considered for investigation for each BVWT prototype - 60 mm and 90 mm.

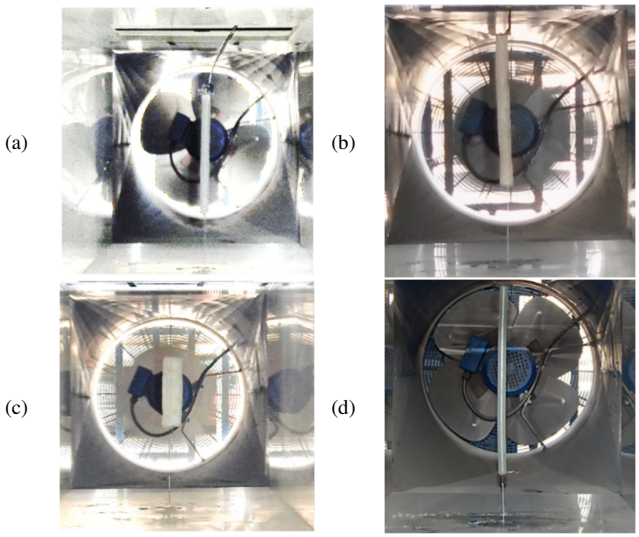

Fig. 1. The manufactured VBWT prototypes with different mast materials: (a) VBWT-GF-14-190, (b) VBWT-PU-14-190, (c) VBWT-PU-28-165, (d) VBWT-PE-11-260.

The manufactured prototypes of VBWTs were tested under a wind tunnel at the Laboratory of Electromechanical Systems (LASEM), as depicted in Figure 2(a). The experimental setup was designed to systematically evaluate the vibrational response of each turbine under varying rod lengths and wind tunnel excitation frequencies. The lower end of the rod in each VBWT prototype was fixed using pressure screws on the support structure. These screws allowed the control of the rod length, as shown in Figure 2(b). The velocity of the wind was measured with an AM 4204 anemometer. A 6-axis MEMS inertial sensor, specifically the MPU-9250 sheet, was used to capture the vibrational acceleration at the mast tip of the VBWT. This sensor can measure the dynamic acceleration caused by vibration and static acceleration, such as gravity, across a three-axis accelerometer and a three-axis gyroscope in a single compact module. This allows the simultaneous measurement of both the linear acceleration and angular velocity along the X, Y, and Z. The data acquisition system used in this study was centered around the Arduino Mega 2560 board (Figure 2(c)), an open-source microcontroller platform based on the ATmega2560 chip.

The experimental procedure, presented in Figure 3, started by calibrating the MPU-9250 accelerometer using a calibration program developed with the Arduino IDE. Then, the rod length, which significantly influences the resonant behavior of the system was adjusted with the control of the pressure screws. Subsequently, the excitation frequency of the wind tunnel was managed to adjust the flow regime corresponding to a desired Reynolds number. To ensure accuracy, the velocity of the airflow was checked with the anemometer. After that, the CoolTerm program was run with a predefined program to capture the acceleration of the VBWT. Finally, a Fast Fourier Transform (FFT) spectrum analysis was carried out to find out the dominant frequencies of vibration. An FFT converts a signal from its original domain, i.e., the time domain, to a representation in the frequency domain and vice versa. So, it splits a signal into different spectral components, and hence offers frequency information about it. The generalized form of an FFT transform, denoted as $Y(n)$, of a discretized signal $(X_k,\ k = 0,..,N-1)$ of size N is written as:

$$Y(n) = \sum_{k=0}^{N-1} X_k \left(\cos\left(\frac{2\pi k}{N} n\right) - i \sin\left(\frac{2\pi k}{N} n\right)\right) \quad (1)$$

III. RESULTS AND DISCUSSION

This section presents the experimental results obtained from the testing of the four VBWT configurations. Each turbine was evaluated under two distinct rod lengths - 60 mm and 90 mm - to assess the impact of structural geometry and material on the dynamic response under various airflow excitations. Figure 4 illustrates the distributions of the measured linear accelerations at the mast tip for all four VBWT configurations for the case of a rod length of 60 mm and a wind velocity of 10 $m.s^{-1}$. The corresponding FFT spectra of these signals are presented in Figure 5. The findings demonstrated that the acceleration fluctuated between positive and negative values, indicating an alternate oscillation of the VBWT. This unsteady behavior was directly linked to the vibrational dynamics of the VBWT, which resulted from the periodic shedding of vortices in the wake region, a phenomenon known as the von Kármán vortex street. The foremost direction of vibrations was orthogonal to the wind direction, consistent with the behavior of the flow past cylindrical or bluff bodies. Table I summarizes the distribution of the Peak Amplitude (*PA*), the frequency (*f*), and the corresponding Standard Deviations (*SD*) for all investigated VBWT cases operating under four different Reynolds numbers (*Re*). The results showed that the SD across multiple tests remained below 10% in most cases for both the peak amplitude and frequency, confirming the credibility and consistency of the experimental methodology.

As previously discussed, the rod length had a significant impact on the vibrational amplitude of the VBWT. Specifically, as the rod length increased from 60 mm to 90 mm, the peak amplitude of vibration raised for all Reynolds numbers. For example, in the case of the VBWT-GF-14-190 turbine, the peak amplitude changed from 0.047 $m.s^{-2}$ to 0.071 $m.s^{-2}$ since the rod length moved from 60 mm to 90 mm. This behavior can be explained by the bending nature of the mechanical solicitation of the rod. If the rod was considered as a beam, its deflection would be greater with an increased beam length. In addition, it can be clearly seen that the peak

frequency decreased with an increasing rod length. For instance, the peak frequency of the VBWT-PU-14-190 turbine changed from 4.018 Hz to 2.894 Hz.

(a)

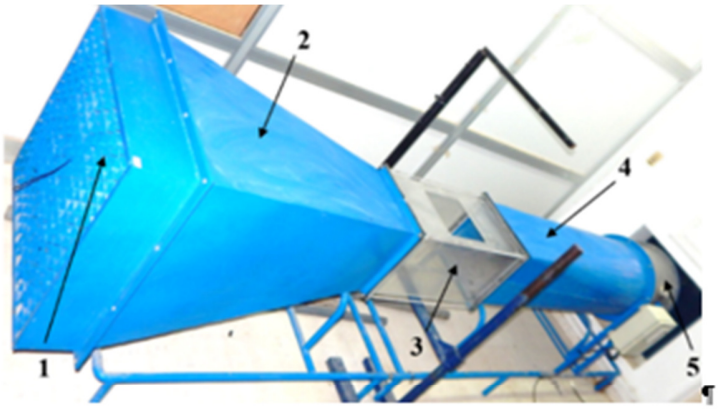

1- Drive section 2- Diffuser 3-Test section 4- Contraction cone 5- Setting chamber

(b)

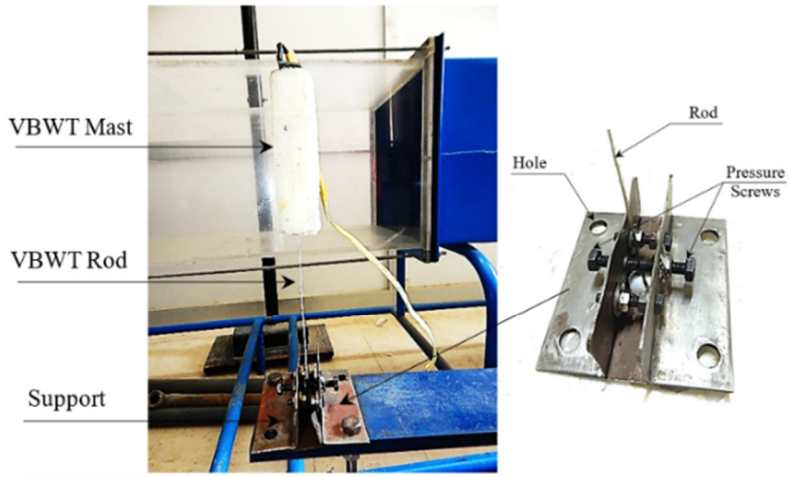

(c)

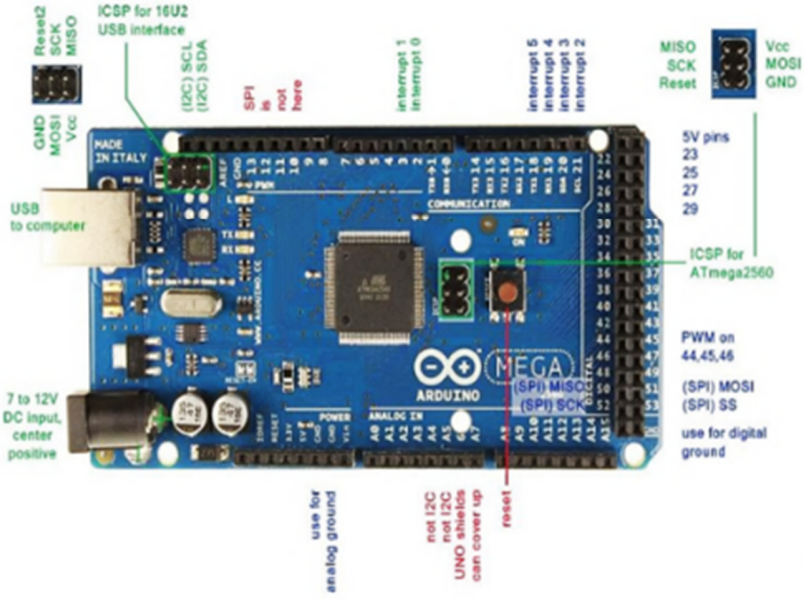

Fig. 2. (a) Wind tunnel, (b) VBWT's installed prototype, and (c) Arduino Mega 2560 card.

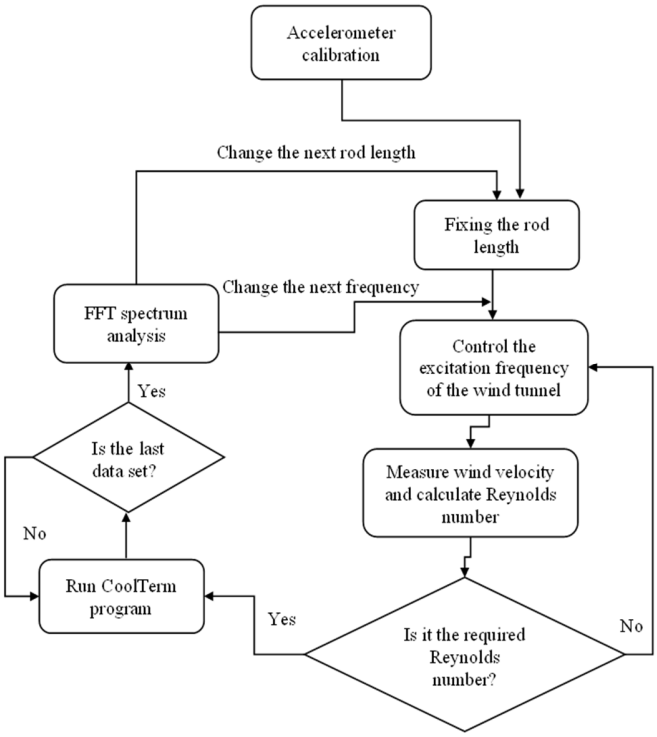

Fig. 3. Experimental procedure flowchart.

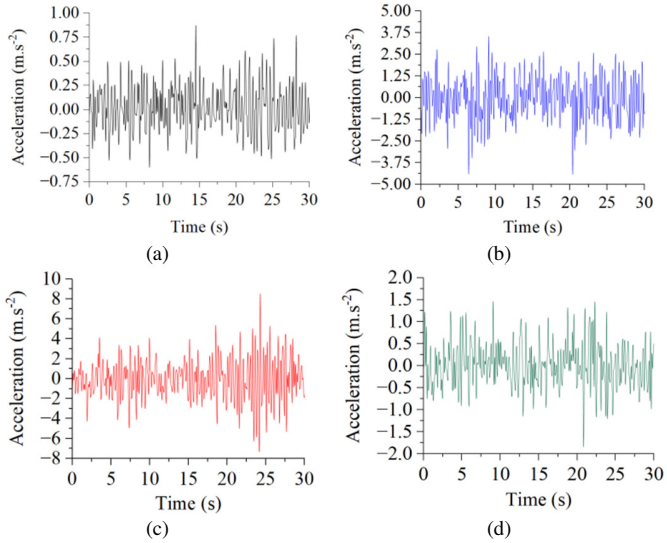

Fig. 4. Temporal evolution of measured acceleration at the mast tip of the VBWT equipped with a rod length of 60 mm. (a) VBWT-GF-14-190, (b) VBWT-PU-14-190, (c) VBWT-PU-28-165, (d) VBWT-PE-11-260.

This observation can be explained by the fact that a longer rod resulted in increased acceleration. With a larger displacement, the VBWT turbine will take longer to complete each oscillation cycle. A comparison between the VBWT-PU-28-165 and VBWT-PU-28-190 prototypes revealed that both the mast diameter and length are key parameters influencing the frequency of vibration and, with a lesser extent, the peak amplitude. For instance, under the same wind tunnel conditions and a rod length of 60 mm, the peak vibration frequencies were 4.018 Hz for the VBWT-PU-14-190 and 3.068 Hz for the VBWT-PU-28-165.

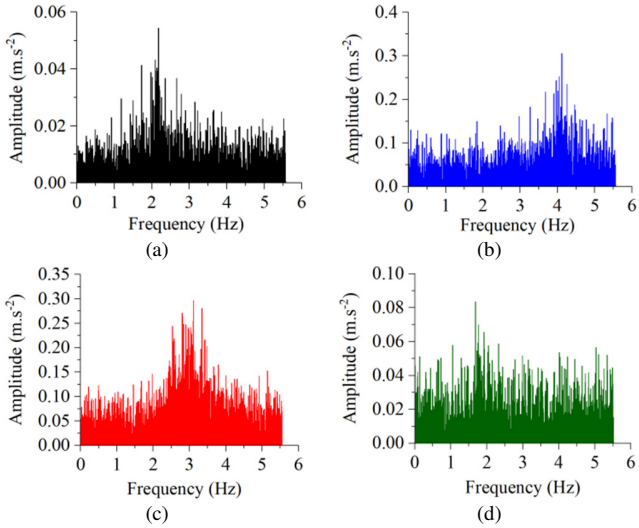

Fig. 5. FFT spectrum of measured acceleration at the mast tip of the VBWT equipped with a rod length of 60 mm. (a) VBWT-GF-14-190, (b) VBWT-PU-14-190, (c) VBWT-PU-28-165, (d) VBWT-PE-11-260.

TABLE I. AN OVERVIEW OF PEAK AMPLITUDE AND FREQUENCY FOR EACH INVESTIGATED CASE

BVWT prototype	**Rod's length, *l* (mm)**	***Re***	***PA*** **(m s^{-2})**	***PA-SD*** **(%)**	***f*** **(Hz)**	***f-SD*** **(%)**
VBWT-GF-14-190	60	5025	0.034	2.71	2.02	1.12
		6282	0.039	3.45	2.09	1.35
		7000	0.054	4.30	2.16	1.23
		7179	0.047	5.51	2.11	1.94
	90	5025	0.066	4.31	1.28	1.55
		6282	0.086	5.32	1.38	1.93
		7000	0.072	7.52	1.34	2.12
		7179	0.071	8.56	1.36	2.51
VBWT-PU-14-190	60	5025	0.160	4.56	4.01	3.76
		6282	0.240	4.35	4.17	3.34
		7000	0.303	5.68	4.13	3.69
		7179	0.221	6.77	4.30	3.96
	90	5025	0.201	6.48	2.89	4.37
		6282	0.335	7.36	2.93	3.39
		7000	0.278	9.44	2.74	5.07
		7179	0.263	10.8	3.09	5.06
VBWT-PU-28-165	60	10739	0.101	3.65	3.06	1.91
		13424	0.152	3.48	2.97	2.02
		14958	0.298	4.76	3.11	1.70
		15342	0.278	6.31	3.10	2.48
	90	10739	0.162	4.62	2.18	1.87
		13424	0.214	6.08	1.94	2.26
		14958	0.220	7.99	1.89	2.68
		15342	0.205	8.62	2.03	2.83
VBWT-PE-11-260	60	4219	0.052	3.97	1.83	2.03
		5273	0.071	3.64	1.76	2.74
		5876	0.085	4.76	1.70	2.58
		6027	0.090	6.58	1.69	2.56
	90	4219	0.062	4.99	1.23	2.82
		5273	0.087	6.76	1.03	3.11
		5876	0.104	8.01	1.06	3.14
		6027	0.176	8.87	1.10	3.40

Furthermore, a comparison between the VBWT-GF-14-190 and VBWT-PU-14-190 prototypes, showed that the mast material exhibited a noticeable impact on both the amplitude and the frequency of vibration. These observations can be described by the fact that the investigated VBWTs were manufactured to operate under the lock-in regime defined by a Strouhal number of nearby 0.2. In this lock-in condition, the frequency of vibration approximately met the natural frequency of the VBWT structure which depends on the VBWT design. The changes in both the peak amplitude and frequency were explained by the inertia effects. Based on these findings, the PU material proposed for the mast demonstrated superior performance in terms of the oscillation frequency and amplitude compared to other materials investigated in [10, 14]

IV. CONCLUSION

In this study, four Vortex Bladeless Wind Turbine (VBWT) prototypes with different mast materials and dimensions were manufactured, tested in a wind tunnel, and analyzed. The mast materials - Glass Fiber (GF), Polyethylene (PE), and Polyurethane (PU) - have not been previously explored or compared in related research. Two rod lengths of 60 mm and 90 mm were examined for all VBWT prototypes.

Based on the experimental results, the following key points are summarized:

- The foremost direction of vibrations was orthogonal to the wind direction, confirming that the resulting vibrations were induced by vortex shedding, known as the phenomenon of the von Kármán vortex street.
- The rod length significantly affected both the peak amplitude and vibration frequency. A longer rod exhibited greater deflection, consistent with the beam bending behavior, leading to larger displacement amplitudes and lower natural frequencies.
- The mast diameter played a key role in determining the frequency of vibration. Specifically, a mast with a diameter of 28 mm resulted in a lower vibration frequency compared to a mast with a diameter of 14 mm.
- The mast material had an important impact on both the amplitude and frequency of vibration. The PU VBWT underwent a larger peak amplitude and greater peak frequency during vibration in comparison with the GF VBWT, which can be attributed to the higher density and mass of GF.
- All tested VBWTs operated within the lock-in regime, characterized by a Strouhal number of around 0.2. In this lock-in condition, the vibration frequency was almost equal to the natural frequency of the structure.

Future work should assess the long-term durability of mast materials under outdoor conditions. Additionally, design improvements and hybrid system integration based on the current findings may further enhance the system's innovation and adaptability.

ACKNOWLEDGMENT

This research work is supported by the PEJC2024-D6P2 project of the Young Researchers Encouragement Program of the Ministry of Higher Education and Scientific Research of Tunisia.

REFERENCES

[1] Q. Hassan *et al.*, "A comprehensive review of international renewable energy growth," *Energy and Built Environment*, Jan. 2024, https://doi.org/10.1016/j.enbenv.2023.12.002.

[2] A. Ketata, Z. Driss, and M. S. Abid, "1D gas dynamic code for performance prediction of one turbocharger radial turbine with different finite difference schemes," *Mechanics & Industry*, vol. 20, no. 6, 2019, Art. no. 627, https://doi.org/10.1051/meca/2019073.

[3] M. Chen, J. Wei, X. Yang, Q. Fu, Q. Wang, and S. Qiao, "Multi-objective optimization of multi-energy complementary systems integrated biomass-solar-wind energy utilization in rural areas," *Energy Conversion and Management*, vol. 323, Jan. 2025, Art. no. 119241, https://doi.org/10.1016/j.enconman.2024.119241.

[4] M. Sun *et al.*, "A novel small-scale H-type Darrieus vertical axis wind turbine manufactured of carbon fiber reinforced composites," *Renewable Energy*, vol. 238, Jan. 2025, Art. no. 121923, https://doi.org/10.1016/j.renene.2024.121923.

[5] M. Pahlavanzadeh, M. Mohammadimehr, M. Irani-Rahaghi, and S. M. Emamat, "Vibration response on the rod of vortex bladeless wind power generator for a sandwich beam with various face sheets and cores based on different boundary conditions," *Mechanics Based Design of Structures and Machines*, vol. 53, no. 3, pp. 1709–1735, 2025, https://doi.org/10.1080/15397734.2024.2391920.

[6] A. Chizfahm, E. A. Yazdi, and M. Eghtesad, "Dynamic modeling of vortex induced vibration wind turbines," *Renewable Energy*, vol. 121, pp. 632–643, Jun. 2018, https://doi.org/10.1016/j.renene.2018.01.038.

[7] A. Tripathi, S. Thakur, and T. Aggarwal, "Modal and Static Analysis of Vortex Bladeless Wind Turbines with Different Geometries," in *15th International Conference on Materials Processing and Characterization (ICMPC 2023)*, Newcastle, England, Sep. 2023, https://doi.org/10.1051/e3sconf/202343001254.

[8] S. S. Dol and H. Hamdan, "Application of Vortex Bladeless Turbines at the offshore Platform for Sustainable Energy," in *ADIPEC*, Abu Dhabi, UAE, Nov. 2024, https://doi.org/10.2118/222566-MS.

[9] A. Das and M. Rahimi, "Effects of Geometry in 2D Simulations for Vortex-Induced Vibration of Bladeless Wind Turbines," *Iranian Journal of Chemistry and Chemical Engineering*, vol. 44, no. 1, pp. 203–215, 2025.

[10] S. Francis, V. Umesh, and S. Shivakumar, "Design and Analysis of Vortex Bladeless Wind Turbine," *Materials Today: Proceedings*, vol. 47, pp. 5584–5588, Jan. 2021, https://doi.org/10.1016/j.matpr.2021.03.469.

[11] S. Francis and A. Swain, "Modelling and harnessing energy from flow-induced vibration, particularly VIV and galloping: An explicit review," *Ocean Engineering*, vol. 312, Nov. 2024, Art. no. 119290, https://doi.org/10.1016/j.oceaneng.2024.119290.

[12] L. O. A. Barata, K. Takahiro, T. Ueno, and L. Hasanudin, "Experimental Investigation of Bladeless Power Generator from Wind-induced Vibration.," *International Journal of Renewable Energy Development*, vol. 11, no. 3, 2022.

[13] G. L. Tenorio, J. Ortega, L. Ortíz, and N. Marín-Calvo, "Stiffness Impact on the Design and Sustainable Functioning of Vortex Bladeless Turbines," in *9th International Engineering, Sciences and Technology Conference (IESTEC)*, Panama City, Panama, Jul. 2024, pp. 210–215, https://doi.org/10.1109/IESTEC62784.2024.10820226.

[14] J. Nejadali, "Design Improvement of the Small-Scale Vortex-Induced Bladeless Wind Turbine Considering the Characteristic Length of the Oscillating Structure," *Iranian Journal of Science and Technology, Transactions of Mechanical Engineering*, vol. 48, no. 4, pp. 1839–1850, 2024, https://doi.org/10.1007/s40997-023-00739-6.

[15] H. Kang, J. Kook, J. Lee, and Y.-K. Kim, "A Novel Small-Scale Bladeless Wind Turbine Using Vortex-Induced Vibration and a Discrete Resonance-Shifting Module," *Applied Sciences*, vol. 14, no. 18, 2024, Art. no. 8217, https://doi.org/10.3390/app14188217.